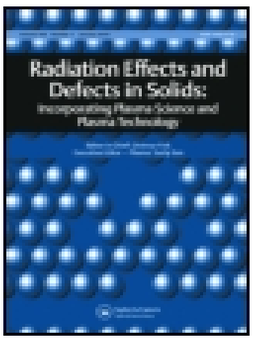

Taylor & Francis
Taylor & Francis Group

Radiation Effects and Defects in Solids
Incorporating Plasma Science and Plasma Technology

ISSN: 1042-0150 (Print) 1029-4953 (Online) Journal homepage: http://www.tandfonline.com/loi/grad20

Synthesis and characterization of graphene quantum dots and their size reduction using swift heavy ion beam

Praveen Mishra & Badekai Ramchandra Bhat

To cite this article: Praveen Mishra & Badekai Ramchandra Bhat (2018): Synthesis and characterization of graphene quantum dots and their size reduction using swift heavy ion beam, Radiation Effects and Defects in Solids, DOI: 10.1080/10420150.2018.1424850

To link to this article: https://doi.org/10.1080/10420150.2018.1424850

Published online: 16 Jan 2018.

Submit your article to this journal

View related articles

View Crossmark data

Full Terms & Conditions of access and use can be found at
http://www.tandfonline.com/action/journalInformation?journalCode=grad20

RADIATION EFFECTS & DEFECTS IN SOLIDS, 2018
https://doi.org/10.1080/10420150.2018.1424850

Taylor & Francis
Taylor & Francis Group

Check for updates

Synthesis and characterization of graphene quantum dots and their size reduction using swift heavy ion beam

Praveen Mishra and Badekai Ramchandra Bhat

Catalysis and Materials Laboratory, Department of Chemistry, National Institute of Technology Karnataka, Surathkal, India

ABSTRACT

Graphene quantum dots (GQDs) are nanosized fragments of graphene displaying quantum confinement effect. They have shown to be prepared from various methods which include ion beam etching of graphene. However, recently the modification of the GQDs has garnered tremendous attention owing to its suitability for various applications. Here, we have studied the effect of swift ion beam irradiation on the properties of GQDs. The ion beam treatment on the GQDs exhibited the change in observed photoluminescence of GQDs as they exhibited a blue luminescence on excitation with long-wave UV ($\approx$365 nm) due to the reduction in size and removal of the ethoxy (–C–O–C–) groups present on the quantum dots. This was confirmed by transmission electron microscopy, particle size analysis, and Fourier transform infrared spectroscopy.

ARTICLE HISTORY
Received 3 December 2017
Accepted 21 December 2017

KEYWORDS
Graphene quantum dots; ion beam; photoluminescence

1. Introduction

Graphene quantum dots (GQDs) are zero-dimensional graphene fragments where the movement of the exciton is confined in all three spatial directions. Unlike graphene, GQDs possesses a finite band gap which along with exciton confinement leads to photoluminescence. The infinite Bohr radius of graphene enables researchers with the ability to tune the photoluminescence of GQDs by varying its size. Kim et al. (*1*) have shown the remarkable correlation between the PL and size of the GQDs within sizes ranging from 12 to 35 nm. GQDs are thus widely used for a variety of applications among which few important ones being photovoltaic devices as shown by Hamilton et al. (*2*), organic light-emitting diodes reported by Tang et al. (*3*), being used in fuel cells by Li et al. (*4*), their applications as sensors which is well complied by Benítez-Martínez and Valcárcel (*5*) and as biosensors by Xie et al. (*6*), and its use in the drug delivery systems presented by Zheng et al. (*7*).

Bacon et al. (*8*) have reviewed that the synthesis of GQDs could be made possible by various routes. As is the case with any nanoparticle, the steps to achieve it are one among the top-down approach or bottom-up approach. The synthesis can also be classified as chemical or physical methods. In terms of yield, the chemical synthesis always is a beneficial route to follow. This mode of synthesis also enables researchers to chemically modify the GQDs to obtain the desired properties, for e.g. Jang et al. (*9*) reported that the oxidation of GQDs

CONTACT Badekai Ramchandra Bhat ram@nitk.edu.in

© 2018 Informa UK Limited, trading as Taylor & Francis Group

results in the red-shift the PL from blue to green. However, a major limitation of the chemical route is the production of non-regular sized GQDs. This in turns limits their usability as it dilutes the property of the dots. Physical route of producing GQDs also have shown better control over the shape and size of the end product. Ponomarenko et al. (*10*) reported the use of ultra-high-resolution electron beam lithography for cutting graphene to desired size fragments. Lee et al. (*11*) demonstrated the fabrication of GQDs using block copolymer as etch mask with good size control. However, low absolute yield was a major drawback in such methods.

The effect of ion beam over graphene is well studied. Kumar et al. (*12*) reported the stability of graphene in high density 150 MeV Au ion irradiation. They reported the occurrence of defects at higher fluence with appreciable retainment of crystallinity. In another report, Kumar et al. (*13*) showed that the swift heavy ion irradiation of 100 MeV Ag ion may be utilized as a tool for defect annealing in graphene. They also observed that a fluence of Ag ion irradiation above 1×10^{13} ions/cm^2 may reduce the number of graphene layers. The use of focused ion beam to cut graphene sheet was reported by Kotakoski et al. (*14*). They used Ga^+ focused ion beam to carve out random patterns from pristine graphene. This study showed how ion beam can be utilized in cleaving the graphene sheet to smaller sizes. However, the effect of ion beam irradiation on graphene oxide was less explored. Tyagi et al. (*15*) reported that structural changes may be brought about by exposing graphene oxide to electron beam. They studied the reduction of graphene oxide in 25 eV electron beam with varying fluence. In the present study, we report a two-step process of producing size-controlled GQDs which make use of both chemical and physical process. Additionally, the reported method is a quintessential top-down method of synthesis which produces blue luminescence GQDs.

2. Materials and methods

Graphite was procured from Sigma Aldrich. Sulfuric acid, nitric acid, phosphoric acid, hydrogen peroxide, hydrochloric acid and sodium hydroxide were purchased from Finar Chemicals and used without further purification.

In a typical synthesis procedure (Figure 1), graphene oxide was prepared using improved Hummer's method as presented by Marcano et al. (*16*). Further, as-prepared graphene oxide was put in a Teflon-lined autoclave in alkaline medium and the reaction was kept for 16 h at 150°C which is in accordance to hydrothermal synthesis reported by Pan et al. (*17*). This

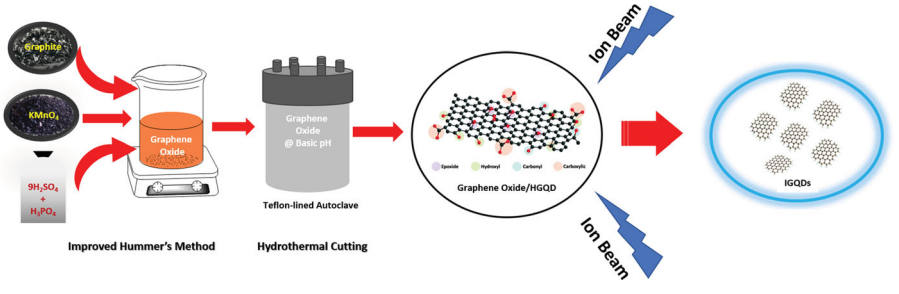

Figure 1. A schematic representation of the synthesis of IGQDs.

yielded a suspension of GO fragments and GQDs. The as-obtained fragmented GO and GQDs were spin coated onto a glass substrate and then exposed to Ni ion beam of 80 MeV at a fluence of 1×10^{12} ions/cm^2 available from the 15 UD tandem pelletron accelerator at IUAC, New Delhi, India. The resultant GQDs were redispersed in water using an ultrasonic bath. The GO was characterized using a Rigaku miniflex X-ray diffractometer using Cu-Kα radiation of 1.54 Å operating at 40 kV and 15 mA with a scan rate of 2°/s. GQDs were characterized using transmission electron microscopy (TEM) (JEM-2100Plus Transmission Electron Microscope), Bruker Alpha Eco-ATR FTIR in ATR mode with a scan range of 4000–600 cm^{-1} and 24 scans, Analytik Jena Specord S600 UV-Vis Spectrophotometer, and Horiba Fluoromax Spectrofluorometer.

3. Results and discussion

GO as synthesized was analyzed using X-ray diffraction. GO represents itself in the XRD with its characteristic broad peak corresponding to the (002) plane found at a diffraction angle (2θ) of 9.98° (Figure 2). The graphitic sharp peak occurring at 2θ of 26° (inset of Figure 2) is absent in XRD pattern of GO which indicates the complete loss in graphitic staking of 2D carbon layers. These assignments of peaks are well established by Stobinski et al. (*18*). Moreover, Kumar et al. (*12*) have also shown that the presence of trace graphene in graphene oxide is not observed in the conventional XRD and can be seen only with synchrotron XRD. A further inspection of GO by TEM (Figure 3) shows a very clear sheet with usual creases found in a typical 2D structure.

After the hydrothermal treatment of GO, we obtained a mixture of fragmented GO and GQDs. The presence of GQDs was confirmed by the faint blue PL which was observed when the obtained mixture was seen under a long wave UV lamp (inset of Figure 4). The hydrothermally obtained and ion beam irradiated GQDs hereon mentioned as HGQDs and IGQDs were further studied under the TEM to understand the changes brought upon by the

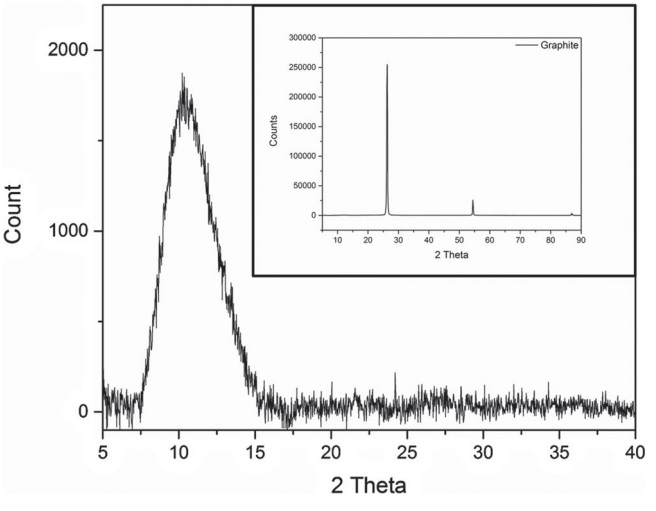

Figure 2. XRD pattern for graphene oxide with spectra of graphite presented as the inset.

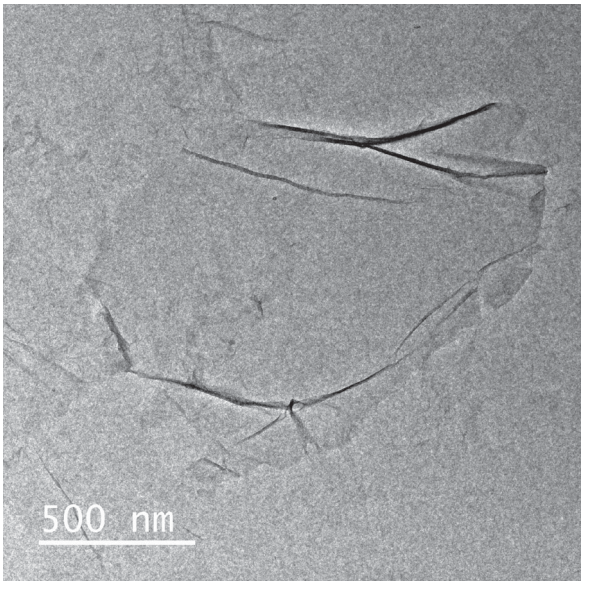

Figure 3. Transmission electron micrograph of graphene oxide.

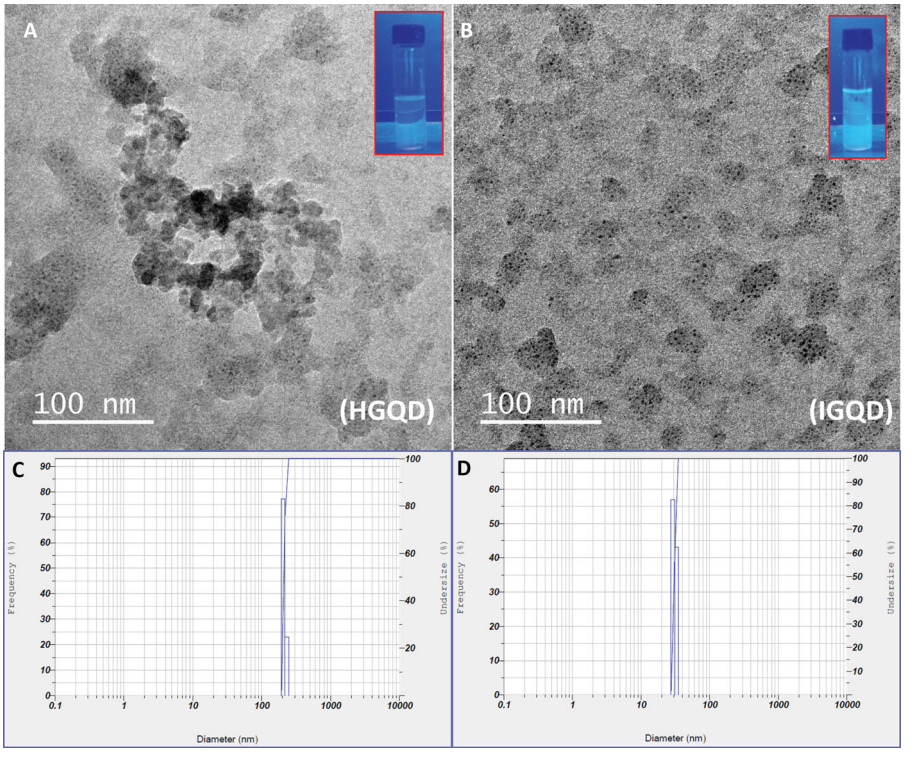

Figure 4. Transmission electron micrograph with visible PL at longwave UV ($\approx$ 365 nm) as inset of (A) HGQD and (B) IGQD; particle size analysis of (C) HGQD and (D) IGQD.

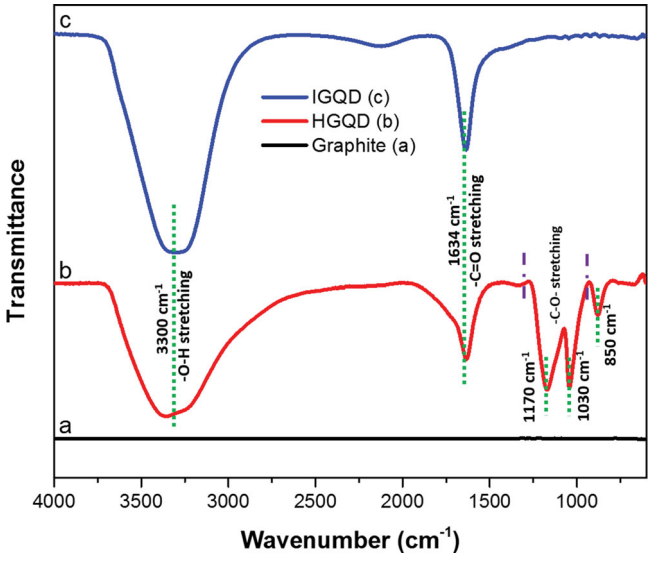

Figure 5. FTIR spectra of graphite, HGQDs, and IGQDs.

irradiation process over their sizes (Figure 4). HGQDs under TEM showed larger a fragment size of 100 nm (which is supported by particle size analysis given in the inset). However, as per the hypothesis, the beam irradiation significantly reduced the size of GQDs as the average size of IGQD was approximately 30 nm (inset from particle size analysis). The reduction in size is brought about due to the cleaving of C–O–C bonds present on the HGQDs and GO when irradiated with the beam. This was well understood by the study of Fourier transform infrared (FTIR) spectra obtained for graphite, HGQDs, and IGQDs (Figure 5). Graphite being devoid of any functional group, showed no peak in the FTIR spectrum. The HGQDs spectrum presented with characteristic peaks corresponded to the –O–H stretching at 3200–3600 cm^{-1}, –C=O stretching at 1634 cm^{-1}, –C–O– stretching at 1000–1300 cm^{-1}, and aromatic –CH substitution at 850 cm^{-1} which are the usual bonds present in GO and HGQDs. However, on irradiating with the ion beam, the –CO– bond cleaved to yield smaller-sized IGQDs, which is evident from the absence of peak corresponding to –C–O– stretching at 1000–1300 cm^{-1} and aromatic CH substitution at 850 cm^{-1} in its FTIR spectrum. The cleaving of the graphene oxide sheet is supposed to be take place along the –C–O–C– bond as shown by Pan et al. (*17*). However, the fragmentation of graphene oxide sheet along –C–O–C– bond takes place where C is substituted with additional H instead of in oxirane configuration as –C–C– bond cleavage is shown to be highly stable in the presence of high-energy irradiation by Kumar et al. (*12*). Additionally, there were no trace peaks corresponding to the Ni–O bond in the FTIR spectra which led us to the conclusion that Ni was not present in the IGQDs and was probably removed as an oxide of nickel.

Photoluminescence is an important property of GQDs as discussed earlier in the introduction. GQDs exhibits PL behavior when the size is reduced below 35 nm. This is due to the fact that the mobility of exciton is restricted in all the direction under 35 nm such that the energy released on the electron hole recombination is in the visible region. However, the energy requirement for the generation of exciton is 3.39 eV which is calculated from the UV–vis spectrometer where GQDs showed the absorbance at 365 nm (Figure 6(a)). It

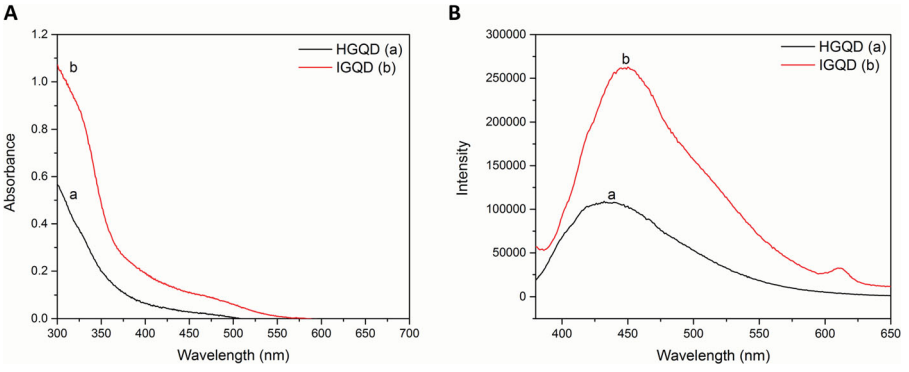

Figure 6. (A) Absorbance spectra and (B) PL spectra of HGQDs and IGQDs.

was expected that IGQDs should emit the higher intensity PL on excitation with 365 nm monochromatic wavelength than that of HGQDs. This is because, the PL is observed due to the presence of graphene quantum dots and, hence, the intensity of PL increases with the increase in the number of quantum dots. The PL spectra of HGQDs and IGQDs agree with this assumption (Figure 6(b)). Moreover, a closer inspection shows a very faint red shift in the emission within the PL from HGQDs from IGQDs. This is due to the better size regularization of GQDs from HGQDs to IGQDs. The size of fragments in HGQDs was very large and also not controlled. They had huge variation which was evident from their transmission electron micrograph. As the PL emission varies with the size of quantum dots, the variation in size leads to a wide band of emission spectrum. However, in case of IGQS, the ion beam irradiation not only reduces the size of the quantum dots, the homogeneous nature of fluence of the radiation means the size of the dots are well regularized thereby giving a comparatively narrower emission spectrum. It must be noted along with this that the regularization of size of GQDs by ion beam also depends on the distribution of ethoxy linkage over the GO and HGQDs frame which is not well controlled in the chemical route. Hence, the overall nature of the emission peak is still very wide as a result. Therefore, the results obtained from PL spectroscopy and TEM analysis suggest that the treatment of GO and HGQD with swift heavy ion beam leads to a successful reduction in the size of the quantum dots.

4. Conclusions

In this study we have synthesized GQDs via hydrothermal cutting of GO sheets which were further reduced in size by means of Ni^{+} ion beam irradiation. High-energy Ni ions were responsible for the cleaving of ethoxy bond present in GO and HGQDs which led to the reduction in size of the GQDs thereby increasing its PL intensity. The PL of the GQDs is a result of excitonic entrapment due to its size reduction. The controlled size distribution of ion beam irradiation of GQDs is evident from the TEM and particle size analysis. Hence, ion beam irradiation can be sought as a suitable technique to reduce the size of GQDs.

Acknowledgements

The authors are thankful to Inter University Accelerator Centre (IUAC), New Delhi, for providing the irradiation facility. The author, Mr Praveen Mishra would like to acknowledge National Institute of Technology Karnataka for extending the infrastructure for research.

Disclosure statement

No potential conflict of interest was reported by the authors.

Funding

Mr Praveen Mishra would like to acknowledge National Institute of Technology Karnataka for the research fellowship.

ORCID

Praveen Mishra http://orcid.org/0000-0002-2132-4499
Badekai Ramachandra Bhat http://orcid.org/0000-0002-8169-1055

References

(1) Kim, S.; Hwang, S.W.; Kim, M.-K.; Shin, D.Y.; Shin, D.H.; Kim, C.O.; Yang, S.B.; Park, J.H.; Hwang, E.; Choi, S.-H., et al. *ACS Nano*. **2012,** *6*, (9), 8203–8208.
(2) Hamilton, I.P.; Li, B.; Yan, X.; Li, L.S. *Nano Lett.*. **2011,** *11*, (4), 1524–1529.
(3) Tang, L.; Ji, R.; Cao, X.; Lin, J.; Jiang, H.; Li, X.; Teng, K.S.; Luk, C.M.; Zeng, S.; Hao, J., et al. *ACS Nano*. **2012,** *6*, (6), 5102–5110.
(4) Li, Y.; Zhao, Y.; Cheng, H.; Hu, Y.; Shi, G.; Dai, L.; Qu, L. *J. Am. Chem. Soc*. **2012,** *134*, (1), 15–18.
(5) Benítez-Martínez, S.; Valcárcel, M. *TrAC Trends Anal. Chem*. **2015,** *72*, 93–113.
(6) Xie, R.; Wang, Z.; Zhou, W.; Liu, Y.; Fan, L.; Li, Y.; Li, X. *Anal. Methods*. **2016,** *8*, (20), 4001–4006.
(7) Zheng, X.T.; He, H.L.; Li, C.M. *RSC Adv.*. **2013,** *3*, (47), 24853–24857.
(8) Bacon, M.; Bradley, S.J.; Nann, T. *Part. Part. Syst. Char*. **2014**, *31*, (4), 415–428.
(9) Jang, M.H.; Ha, H.D.; Lee, E.S.; Liu, F.; Kim, Y.H.; Seo, T.S.; Cho, Y.H. *Small*. **2015,** *11*, (31), 3773–3781.
(10) Ponomarenko, L.A.; Schedin, F.; Katsnelson, M.I.; Yang, R.; Hill, E.W.; Novoselov, K.S.; Geim, A.K. *Science*. **2008,** *320*, (5874), 356–358.
(11) Lee, J.; Kim, K.; Park, W.I.; Kim, B.-H.; Park, J.H.; Kim, T.-H.; Bong, S.; Kim, C.-H.; Chae, G.; Jun, M., et al. *Nano Lett.Lett*. **2012,** *12*, (12), 6078–6083.
(12) Kumar, S.; Tripathi, A.; Khan, S.A.; Pannu, C.; Avasthi, D.K. *Appl. Phys. Lett*. **2014,** *105*, (13), 133107.
(13) Kumar, S.; Tripathi, A.; Singh, F.; Khan, S.A.; Baranwal, V.; Avasthi, D.K. *Nanoscale Res, Lett*. **2014,** *9*, (1), 126.
(14) Kotakoski, J.; Brand, C.; Lilach, Y.; Cheshnovsky, O.; Mangler, C.; Arndt, M.; Meyer, J.C. *Nano Lett.Lett*. **2015,** *15*, (9), 5944–5949.
(15) Tyagi, C.; Lakshmi, G.B.V.S.; Kumar, S.; Tripathi, A.; Avasthi, D.K. *Nucl. Instrum. Meth B*. **2016,** *379*, (Supplement C), 171–175.
(16) Marcano, D.C.; Kosynkin, D.V.; Berlin, J.M.; Sinitskii, A.; Sun, Z.; Slesarev, A.; Alemany, L.B.; Lu, W.; Tour, J.M.. *ACS Nano*. **2010,** *4*, (8), 4806–4814.
(17) Pan, D.; Zhang, J.; Li, Z.; Wu, M. *Adv. Mater*. **2010,** *22*, (6), 734–738.
(18) Stobinski, L.; Lesiak, B.; Malolepszy, A.; Mazurkiewicz, M.; Mierzwa, B.; Zemek, J.; Jiricek, P.; Bieloshapka, I. *J. Electron. Spectrosc*. **2014,** *195*, (Supplement C), 145–154.